Beyond Bragg mirrors: the design of aperiodic omnidirectional multilayer reflectors

2011 J. Phys. A: Math. Theor. 44 035005

(http://iopscience.iop.org/1751-8121/44/3/035005)

J. Phys. A: Math. Theor. **44** (2011) 035005 (9pp) doi:10.1088/1751-8113/44/3/035005

Beyond Bragg mirrors: the design of aperiodic omnidirectional multilayer reflectors

Françoise Axel[1] **and Jacques Peyrière**[2]

[1] Laboratoire de Physique des Solides, CNRS-UMR8502 and Université Paris-Sud, Bâtiment 510, 91405 Orsay Cedex, France
[2] Laboratoire de Mathématiques, CNRS-UMR8628 and Université Paris-Sud, Bâtiment 425, 91405 Orsay Cedex, France

E-mail: axel@lps.u-psud.fr and Jacques.Peyriere@math.u-psud.fr

Received 4 August 2010, in final form 22 November 2010
Published 16 December 2010
Online at stacks.iop.org/JPhysA/44/035005

Abstract

A new method that enables omnidirectional reflectivity for all polarizations of incident light over a wide selectable range of wavelengths was used to design aperiodic multilayer mirrors. Choosing the materials, and with the desired threshold value of the reflection coefficient also being given, the resulting reflectors work for all polarizations in a predetermined range of incidence angles and wavelengths. They are 1D photonic aperiodic crystals composed of a stack of layers arranged according to a deterministic aperiodic substitutive sequence appropriately determined. In the calculation of the optical multilayer properties with the Rayleigh–Abeles matrices, the use of the computationally efficient building block recurrence or trace–antitrace map techniques avoids numerical instability and strongly reduces computational time. Experimental measurements of a prototype satisfying predetermined requirements fabricated after the sequence generated by $\sigma:(a, b)\rightarrow(bba, bbba)$ show excellent agreement.

PACS numbers: 68.65.Ac, 78.67.Pt, 42.60.By, 42.79.Fm
Mathematics Subject Classification: 11B85, 20F10, 20M05, 68Q70, 68R15

1. Introduction

The design of highly efficient mirrors is one of the most challenging episodes in the fight for the control of light propagation. Age-old metallic mirrors, which are omnidirectional, absorb light particularly in the infrared and this fact has led, in order to avoid such a drawback, to the search of new structures made of different materials and offering complete gaps.

Among 1D photonic crystals [1, 2] made of a multilayer heterostructure, the most studied are periodic stacks of two kinds of layers ('Bragg mirrors') with, usually, indices n_j and thicknesses d_j adjusted to be $d_j = \lambda/4n_j$, where λ is the wavelength of incident light [3, 4].

The limitations of such periodic structures are due, in particular, to the above constraints on the variation of the relevant heterostructure parameters, which may hamper the design of fully omnidirectional mirrors meeting predetermined specifications, for which wide applications in optical and microwave systems, microcavity laser physics, vertical cavity surface emitting lasers (vcsel), as antenna substrates, coaxial waveguides, angular filters, etc exist [5–7].

The reflectivity of periodic stacks—made for instance of microscope slides or viewgraphs—having spaces between interfaces with random thicknesses arises from Anderson localization [8], unlike what is presented below.

Here, a new general method to design multilayer omnidirectional reflectors is presented. Choosing the materials, and with the desired threshold value of the reflection coefficient also being given, the resulting mirrors work for all polarizations of the incident light in a predetermined range of incidence angles and wavelengths. They are 1D photonic aperiodic crystals composed of a stack of layers arranged according to a deterministic aperiodic substitutive sequence appropriately determined to this end. The optical multilayer properties are calculated with no *a priori* restriction on the heterostructure parameters imposed and without approximations with the Rayleigh–Abeles matrices comprising the physical parameters of each layer. The use of the computationally efficient building block recurrence (BBR) or trace–antitrace map techniques avoids numerical instability and strongly reduces computational time. Experimental tests of a prototype fabricated along these lines show excellent agreement.

2. Framework

A substitutive sequence is the result of the action of a substitution operator σ on the elements of an alphabet **A** composed of two or more letters, in the example presented below and for the prototype made of two letters a and b. These letters represent *heterostructure* layers which differ by their thickness and/or composition. To define σ one defines words of substitution for each letter of the alphabet, for instance aab and ba. Starting then from the word $w_0 = a$, the effect of the application of this example substitution σ:(a,b)→(aab, ba) on the word w_0 is the replacement of each a by aab and of each b by ba. One then gets the word $w_1 = \sigma(w_0) = aab$. Iterating this operation on w_1, one obtains the word $w_2 = \sigma(w_1) = \sigma^2(w_0) = aabaabba$, iterating this operation on w_2, one obtains the word $w_3 = \sigma(w_2) = \sigma^3(w_0) = aabaabbaaabaabbabaaab$, and so on. The same can be done starting with the word $w_0 = b$.

With each substitution σ is associated a matrix M_σ which relates the composition of the sequence obtained after n applications of σ to the composition of the sequence obtained after n–1 applications. In the present example

$$M_\sigma = \begin{pmatrix} 2 & 1 \\ 1 & 1 \end{pmatrix},$$

because $\sigma_a = aab$ acting on a yields two letters a and one letter b, hence the first column of M_σ; $\sigma_b = ba$ acting on b yields one letter b and one letter a, hence the second column of M_σ.

M_σ has one positive eigenvalue ρ larger than all the other ones, which in the present example is $\rho = (3 + \sqrt{5})/2$; the length l_n of the word $w_n = \sigma^n(w_0)$ obtained after n substitutions σ from the word w_0 is of the order of ρ^n.

The lengths (number of letters) of the words w_0, w_1, w_2, w_3, w_4, w_5, w_6, w_7, w_8, w_9, w_{10}, w_{11}, w_{12}, etc are easily found to be respectively 1, 3, 8, 21, 55, 144, 377, 987, 2584, 6765, 17711, 46368, 121393, etc which increase very rapidly with the number of iterations performed. If one now identifies one letter of the alphabet with one type of layer, the very

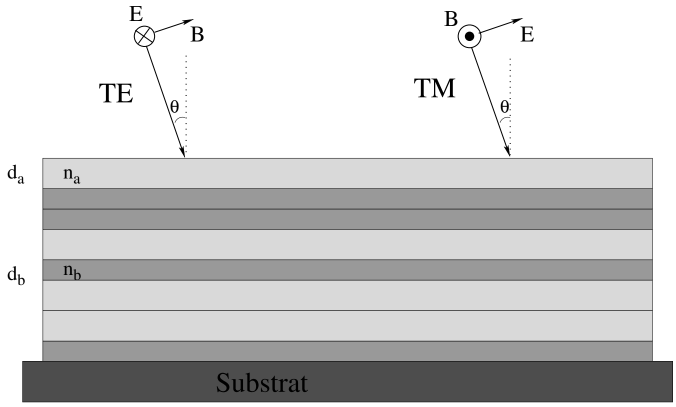

Figure 1. Aperiodic multilayer reflector with layer parameters (see the text) and the electromagnetic mode convention with E and B the electric and magnetic fields respectively.

same applies to the number of layers forming the heterostructure generated using a substitutive sequence. For more details, the reader is referred to [9].

To calculate the optical properties of such a multilayer, one uses the (2×2 in the present case) Rayleigh–Abeles transfer matrices rigorously derived from Maxwell equations which completely characterize light propagation in stratified media [10–12]. The calculations are conducted without approximations. In the set-up with light coming from the air (schematically depicted in figure 1), there is no total reflection at layer interfaces.

With each layer j of the heterostructure (j from 1 to N, N is the total number of layers), assumed to be non-absorbing, isotropic and homogeneous with sharp interfaces infinite in extent, is associated the elementary unimodular Abeles transfer matrix S_j integrating its physical characteristics together with the characteristics of the light which goes through it:

$$S^a = \begin{pmatrix} \cos(2\pi n_a d_a \cos(\theta_a)/\lambda) & (1/p_a)\sin(2\pi n_a d_a \cos(\theta_a)/\lambda) \\ p_a \sin(2\pi n_a d_a \cos(\theta_a)/\lambda) & \cos(2\pi n_a d_a \cos(\theta_a)/\lambda \end{pmatrix}, \tag{1}$$

where λ is the wavelength of incident light, θ_j is the refraction angle in layer j, n_j is the refraction index of layer j, d_j is its thickness and $p_j = n_j \cos(\theta_j)$ for the fundamental 'transverse electric' (TE or s) wave with the electric field E polarized perpendicularly to the incidence plane, and $p_j = \cos(\theta_j)/n_j$ for the fundamental 'transverse magnetic' (TM or p) wave with the magnetic field M polarized perpendicularly to the incidence plane.

The transfer matrix of the whole heterostructure M_n is then

$$M_N = S_N S_{N-1}\, S_{N-2} \ldots . S_2\, S_1. \tag{2}$$

It has been shown in the case of the Fibonacci sequence [13, 14] and then in specific sequences like the Thue–Morse sequence [15]—but this result is general [11, 16]—that the multilayer transmission coefficient can be simply expressed as a function of the sum of the squares of the elements of M_N, which in turn are simple functions of Tr M_N (the sum of diagonal elements) and of aTr M_N (the antitrace or the difference of the two off-diagonal elements) as

$$T = 4/((\mathrm{Tr}\, M_N)^2 + (\mathrm{aTr}\, M_N)^2). \tag{3}$$

Normally then, M_n is obtained by N–1 multiplications of the elementary transfer matrices S_j, which may, in certain configurations, produce an accumulation of rounding errors that can result in numerical instability and deprive the calculation result of its validity. Much effort has been devoted to the search for calculation methods adapted to the solution of such failures in specific situations [17–19].

The BBR method described below stems naturally from the use of substitutive sequences and provides, in the present case, an efficient cure for such difficulties.

3. BBR method

With layer a (GaAs in the experiment) is associated the 2×2 square unimodular matrix A_0 which integrates all of the layer physical parameters, thickness, refraction index and the light parameters, incidence angle, wavelength and mode (TE or TM). In an analogous fashion, with layer b (AlAs in the experiment) can be associated the 2×2 square unimodular matrix B_0.

If in the word $\sigma^j(a)$ where $0 \leqslant j \leqslant n$, one replaces the letter a by the matrix A_0 and the letter b by the matrix B_0, then the resulting matrix product is $A_{j.}$. Similarly, if one makes these associations in the word $\sigma^j(b)$ where $0 \leqslant j \leqslant n$, one obtains the matrix $B_{j.}$.

Let us call A_n and B_n the matrices resulting from n iterations of substitution σ; the BBR allows a simple exact calculation of A_{n+1} and B_{n+1}, when one knows A_n and B_n.

Let us return to the above example with $\sigma(a) = aab$ and $\sigma(b) = ba$. One may write $A_{n+1} = A_nA_nB_n$ and $B_{n+1} = A_nB_n$. Then, to calculate A_{n+1} and B_{n+1} knowing A_n and B_n with the BBR method, only three products of 2×2 matrices are needed, and to calculate A_n and B_n knowing A_0 and B_0, only $3n$ products of 2×2 matrices are needed.

Then the matrix A_n represents the heterostructure having N layers obtained after n iterations of σ. It is identical with M_N defined above.

With the direct product method, in this example, for $n = 7$ iterations M_N is the product of 987 elementary transfer matrices; one then has to calculate 986 products; while with the BBR method one has only $7 \times 3 = 21$ products to calculate, which is a diminution of almost 50 in calculation time. In the general case, a direct product calculation requires of the order of ρ^n products of 2×2 matrices with ρ defined above while with the BBR method only of the order of n products are necessary.

The use of this method enables the possibility of testing a very large number of configurations by varying the deterministic aperiodic substitution, the relevant number of iterations, layer thicknesses and the sequences thus obtained, to sort one generating the omnidirectional mirror answering the prescribed characteristics, within a reasonable amount of calculation time and with excellent accuracy.

4. Trace–antitrace map method

We can describe yet another method of the same order of complexity as BBR to compute the global transfer matrix M_N using trace maps, which in a few cases may even slightly improve on the BBR.

It relies on the remark that, with the same notations as above, A_{n+1} and B_{n+1} are linear combinations of matrices I (unit matrix of order 2), A_n, B_n and $A_n\,B_n$ [20–26]; indeed there exists a 3×4 matrix N_σ, associated with substitutive sequence σ having coefficients $N_{\sigma,i,j}$ (with $1 \leqslant i \leqslant 3$ and $1 \leqslant j \leqslant 4$) which are polynomials of the three variables x, y and z with integer coefficients. With Tr $A_n = x_n$, Tr $B_n = y_n$, and Tr $A_nB_n = z_n$ respectively the trace of matrix A_n, the trace of matrix B_n, and the trace of the matrix product A_nB_n, we can write

$$\begin{pmatrix} A_{n+1} \\ B_{n+1} \\ A_{n+1}B_{n+1} \end{pmatrix} = N_\sigma(x_n, y_n, z_n) \begin{pmatrix} I \\ A_n \\ B_n \\ A_nB_n \end{pmatrix}, \tag{4a}$$

and, with *the same* 3×4 matrix $N_\sigma\ (x_n, y_n, z_n)$,

$$\begin{pmatrix} x_{n+1} \\ y_{n+1} \\ z_{n+1} \end{pmatrix} = N_\sigma\ (x_n, y_n, z_n) \begin{pmatrix} 2 \\ x_n \\ y_n \\ z_n \end{pmatrix}. \tag{4b}$$

For the antitrace, aTr:

$$\begin{pmatrix} \text{aTr } A_{n+1} \\ \text{aTr } B_{n+1} \\ \text{aTr } A_{n+1}B_{n+1} \end{pmatrix} = N_\sigma\ (x_n, y_n, z_n) \begin{pmatrix} 0 \\ \text{aTr } A_n \\ \text{aTr } B_n \\ \text{aTr } A_nB_n \end{pmatrix}. \tag{4c}$$

With this formalism, our example reads

$$\begin{cases} A_{n+1} = -B_n + x_nA_nB_n \\ B_{n+1} = (z_n - x_ny_n) * I + y_nA_n + x_nB_n - A_nB_n \\ A_{n+1}B_{n+1} = (x_n - y_nz_n) * I + \left(x_ny_nz_n - x_n^2 - y_n^2 + 1\right)A_n + y_nA_nB_n \end{cases}, \tag{5}$$

and

$$N_\sigma\ (x_n, y_n, z_n) = \begin{pmatrix} 0 & 0 & -1 & x_n \\ z_n - x_n & y_n & x_n & -1 \\ x_n - y_nz_n & x_ny_nz_n - x_n^2 - y_n^2 + 1 & 0 & y_n \end{pmatrix}. \tag{6}$$

Both of these techniques can be generalized to substitutions operating on a k letter alphabet $\{a_1, a_2, \ldots, a_k\}$. The different letters then represent k heterostructure layers that can be different. But as soon as $k \geqslant 3$, the BBR method is easier to implement and more efficient than the trace map method with trace and antitrace, even if one uses the smallest number of terms according to [23, 24].

Both tools enable us to calculate simply the optical properties of interest of deterministic aperiodic configurations—here the transmission coefficient—and test their ability to become fully omnidirectional mirrors meeting predetermined specifications, with a calculation time which remains reasonable in view of the power currently available from computing facilities, and with excellent accuracy.

Also, they can be used for instance to require omnidirectionality within a prescribed range of incidence angles if one wants to obtain an angular filter. It can be seen that our method allows a large flexibility in parameter selection, in particular wavelength.

In the example of [8], a stack with spaces between interfaces having random thicknesses, the boundaries of the wavelength range where reflectivity can take place are essentially determined on one side by the standard deviation of the spacing roughness (equation (7) of [8]) and on the other by the onset of absorption (equation (13) of [8]). Experiments and calculations are performed for normal incidence. The set-up total thickness is of the order of centimeters, while for the multilayers presented here it is of the order of microns.

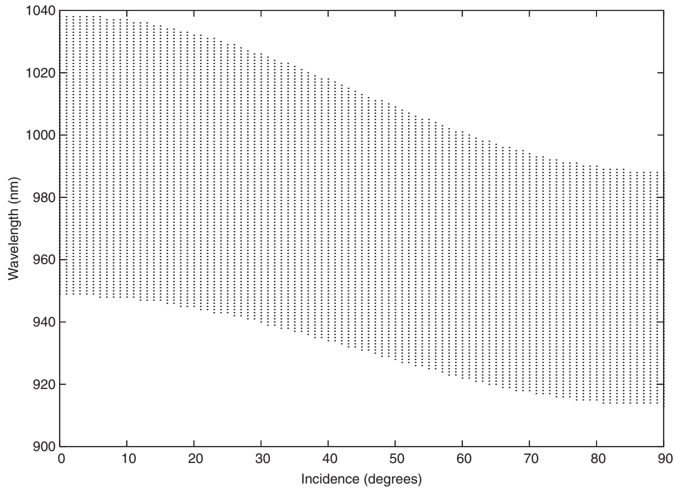

Figure 2. Prototype mirror gap width as a function of incidence: in the dotted area, T (equation (3)) is less than 0.5% for TE and TM modes.

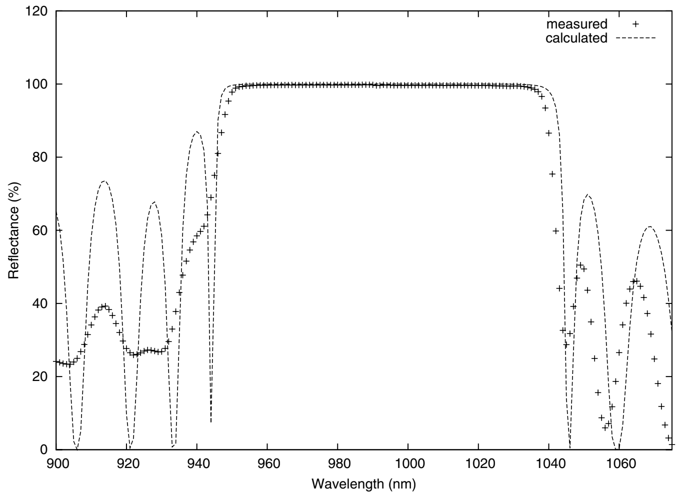

Figure 3. Reflectance of the prototype aperiodic multilayer omnidirectional mirror at normal incidence with unpolarized light as a function of wavelength (nm): calculated (dashed line) and measured (+).

5. Application of the design method and concluding remarks

Multilayer aperiodic lattices have been grown (in particular by molecular beam epitaxy) and investigated by a variety of techniques since the mid-1980s [27–30]. Before the present study however, the search for aperiodic multilayer omnidirectional mirrors with aperiodic substitutive sequences had been limited to the use of a few specific ones, e.g. Fibonacci, Thue–Morse, etc, and their generalizations [31–33].

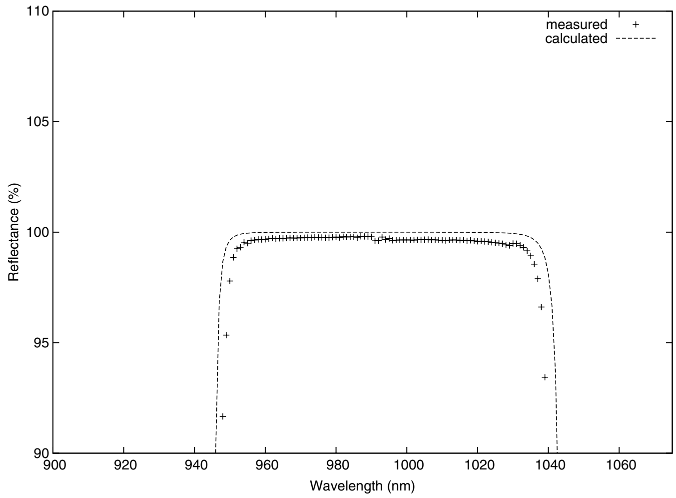

Figure 4. Detail of figure 3.

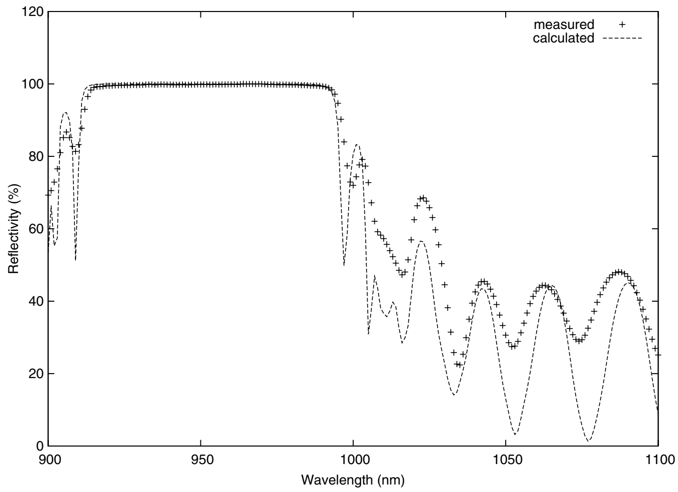

Figure 5. Reflectance of the prototype mirror at 70° incidence with unpolarized light as a function of wavelength (nm): calculated (dashed line) and measured (+). The measured data are corrected to take into account the properties of the gold mirror standard.

We calculated a prototype mirror made of GaAs–AlAs layers after the following specifications: total thickness less than 10 μ, total thickness of AlAs less than 3μ, reflecting better than 99.5% in the range 960–1000 nm where these materials are lossless.

The aperiodic sequence generated by four iterations of $\sigma : (a,b) \to (bba, bbba)$ was found to enable the determination and subsequent fabrication of a prototype 6.3μ thick on a GaAs substrate meeting the requirements, made of GaAs layers 47 lattice constant (0.5645 nm) thick and of AlAs layers 142 lattice constant (0.5661 nm) thick.

The calculated gap width as a function of the incidence angle is shown in figure 2: in the shaded area, T (equation (3)) is less than 0.5% for TE and TM modes. The complete gap has sharp and well-defined boundaries; its width can be estimated to be about 40 nm.

The mirror wafer was made by metal organic chemical vapor deposition by I Sagnes, G Beaudouin and J-Y Marzin at LPN-CNRS, Marcoussis, France. We measured its reflection coefficient at LULI, Ecole Polytechnique, Palaiseau, France, using a Varian CARY500 spectrophotometer equipped with VW and variable angle specular reflectance accessory (VASRA) (to which L Leconte and M Chateau introduced us). Measurements with the VASRA were performed using a gold standard and corrected accordingly.

Experimental procedures and complete results will be published separately elsewhere [34]. Figures 3–5 show the comparison between calculated and measured prototype reflectance; the agreement is excellent.

Acknowledgments

The authors thank P Chavel (IOGS, Palaiseau, France), C Colliex (LPS, Orsay, France) and M Cuniot-Ponsard (IOGS, Palaiseau, France) for stimulating discussions, and the referees for their valuable comments and suggestions.

References

[1] Fink Y, Winn J N, Fan S, Chen C, Michel J, Joannopoulos J D and Thomas E L 1998 A dielectric omnidirectional reflector *Science* **282** 1679
[2] Joannopoulos J D, Meade R D and Winn J N 1995 *Photonic Crystals* (Princeton, NJ: Princeton University Press)
[3] Bruyant A, Lérondel G, Reece P G and Gal M 2003 All-silicon omnidirectional mirrors based on one-dimensional photonic crystals *Appl. Phys. Lett.* **82** 3227
[4] Park Y, Roh Y-G, Cho C-O, Jeon H, Sung M G and Woo J C 2003 GaAs-based near-infrared omnidirectional reflector *Appl. Phys. Lett.* **82** 2770
[5] Dowling J P 1988 Mirror on the wall: you're omnidirectional after all *Science* **282** 1841
[6] Cregan R F, Mangan B J, Knight J C, Birks T A, Russell P St J, Roberts P J and Allan D C 1999 Single-mode photonic band gap guidance of light in air *Science* **285** 1537
[7] Ibanescu M, Fink Y, Fan S, Thomas E L and Joannopoulos J D 2000 An all-dielectric coaxial waveguide *Science* **289** 415
[8] Berry M V and Klein S 1997 Transparent mirrors: rays, waves and localization *Eur. J. Phys.* **18** 222–8
[9] Axel F and Gratias D 1995 *Beyond Quasicrystals* (Paris/Berlin: Les Editions de Physique/Springer)
[10] Rayleigh Lord 1912 On the propagation of waves through a stratified medium, with special reference to the question of reflection *Proc. R. Soc.* **86 A** 207–26
[11] Abeles F 1950 Recherche sur la propagation des ondes electromagnétiques sinusoïdales dans les milieux stratifiés. Application aux couches minces *Ann. Phys.* **5** 596–640
Abeles F 1950 Recherche sur la propagation des ondes electromagnétiques sinusoïdales dans les milieux stratifiés. Application aux couches minces *Ann. Phys.* **5** 707–82
Born M and Wolf E 2006 *Principles of Optics* (Cambridge: Cambridge University Press) chapter 1.6
[12] Yeh P 1988 *Optical Waves in Layered Media* (New York: Wiley)
[13] Kohmoto M, Kadanoff L P and Tang C 1983 Localization problem in one dimension: mapping and escape *Phys. Rev. Lett.* **50** 1870
[14] Kohmoto M, Sutherland B and Iguchi K 1987 Localization in optics: quasiperiodic media *Phys. Rev. Lett.* **58** 2436
[15] Liu N-H 1997 Propagation of light waves in Thue–Morse dielectric multilayers *Phys. Rev.* B **55** 3543
[16] Bendickson J M, Dowling J P and Scalora M 1966 Analytic expressions for the electromagnetic mode density in finite, one-dimensional, photonic band-gap structures *Phys. Rev.* E **53** 4107
[17] Schwartz C and DeSandre L F 1987 New calculational technique for multilayer stacks *Appl. Opt.* **26** 3140
[18] Tan E L 2006 Enhanced R-matrix algorithms for multilayered diffraction gratings *Appl. Opt.* **45** 4803
[19] Ko D Y K and Sambles J R 1988 Scattering matrix method for propagation of radiation in stratified media: attenuated total reflection studies of liquid crystals *J. Opt. Soc. Am.* A **5** 1863–6
[20] Horowitz R D 1975 Induced automorphism on Fricke characters of free groups *Trans. Am. Math. Soc.* **208** 41–50
[21] Allouche J-P and Peyrière J 1986 Sur une formule de récurrence sur les traces de produits de matrices associés à certaines substitutions *C. R. Acad. Sci., Paris* **302** (Série II) 1135

[22] Peyrière J 1991 On the trace map for products of matrices associated with substitutive sequences *J. Stat. Phys.* **62** 411 (see also Course 16 in [9].)

[23] Avishai Y, Berend D and Tkachenko V 1997 Trace maps *Int. J. Mod. Phys.* B **11** 3525–42

[24] Peyrière J 2000 On an article by W. Magnus on the Fricke characters of free groups *J. Algebra* **228** 659–73

[25] Peyrière J 2002 Polynomial dynamical systems associated with substitutions *Substitutions in Dynamics, Arithmetics and Combinatorics (Lecture Notes in Mathematics* no 1794*)* (Berlin: Springer) p 328 chapter 10

[26] Wang X, Grimm U and Schreiber M 2000 Trace and antitrace maps for aperiodic sequences: extensions and applications *Phys. Rev.* B **62** 14020–31

[27] Merlin R, Bajema K, Clarke R, Juang F Y and Bhattacharya P K 1985 Quasiperiodic GaAl–AlAs heterostructures *Phys. Rev. Lett.* **55** 1768

[28] Cheng Z, Savit R and Merlin R 1988 Structure and electronic properties of Thue–Morse lattices *Phys. Rev.* B **37** 4375

[29] Axel F and Terauchi H 1991 High resolution x ray diffraction spectra of Thue–Morse GaAs–AlAs heterostructures: towards a novel description of disorder *Phys. Rev. Lett.* **66** 2223

[30] Steurer W and Sutter-Widmer D 2007 Photonic and phononic quasicrystals *J. Phys. D: Appl. Phys.* **40** R229

[31] Dal Negro L, Stolfi M, Yi Y, Michel J, Duan X, KImerling L C, LeBlanc J and Haavisto J 2004 Photon band gap properties and omnidirectional reflectance in Si/SiO_2 Thue–Morse quasicrystals *Appl. Phys. Lett.* **84** 5186

[32] Qiu F, Peng R W, Huang X Q, Hu X F, Wang Mu, Hu A, Jiang S S and Feng D 2004 Omnidirectional reflection of electromagnetic waves on Thue–Morse dielectric multilayers *Europhys. Lett.* **68** 658

[33] Moretti L, Rea I, Rotiroti L, Rendina I, Abbate G, Marino A and De Stefano L 2006 Photonic band gaps analysis of Thue–Morse multilayers made of porous silicon *Opt. Express* **14** 6264

[34] Axel F, Beaudouin G, Chateau M, Leconte L, Marzin J-Y, Peyrière J and Sagnes I (in preparation)